

# Manifestation of three-body forces in $f_{7/2}$ -shell nuclei.

Alexander Volya

Department of Physics, Florida State University, Tallahassee, FL 32306-4350, USA

(Dated: February 7, 2019)

The traditional nuclear shell model approach is extended to include many-body forces. The empirical Hamiltonian with a three-body force is constructed for the proton and neutron  $0f_{7/2}$  shells. Manifestations of the three-body force in spectra, binding energies, seniority mixing, particle-hole symmetry, electromagnetic and particle transition rates are investigated. The model with a three-body force is demonstrated to provide a better agreement with observations as compared to large-scale traditional shell model calculations.

PACS numbers: 21.45.Ff, 21.60.Cs, 21.30.-x

The many-body problem is central for modern physics. A path from understanding interactions between fundamental constituencies to the diverse physics of the whole system is non-trivial and involves various entangled routes. Among numerous issues, the questions of forces, effective or bare, their hierarchy and renormalizations are of a particular importance. Nuclear physics is a valuable natural arena to explore this.

Microscopic treatments provide a remarkably accurate description of light nuclei based on the observed, bare, two-nucleon interactions [1]. The same calculations indicate that the role of three-body forces is increasingly large and non-perturbative for heavier systems. The many-body approaches with roots in effective interactions from mean-field (one-body) to shell model (one and two-body) indicate a need in empirical many-body force [2, 3, 4]. It is established that, regardless of ab-initio interactions, work in restricted space always gives rise to many-body forces, moreover renormalizations may successfully set the hierarchy of importance[5, 6].

The goal of this work is to examine three-body forces within the nuclear shell model (SM) approach. This includes determination of effective interaction parameters, study of hierarchy in strength from single-particle (s.p.) to two-body to three-body and beyond, manifestations in energy spectra and transitions rates, comparison with different traditional SM calculations and overall assessment for the need of beyond-two-body SM. Previous works in this direction have shown improved description of energy spectra in p-shell nuclei [2, 3] and the significance of three-body monopole renormalizations [4].

The effective interaction Hamiltonian is a sum  $H_k = \sum_{n=1}^k H^{(n)}$  where the  $n$ -body rotationally invariant part is

$$H^{(n)} = \sum_{\alpha\beta} \sum_L V_L^{(n)}(\alpha\beta) \sum_{M=-L}^L T_{LM}^{(n)\dagger}(\alpha) T_{LM}^{(n)}(\beta), \quad (1)$$

the isospin label is omitted here for the sake of simplicity. The operators  $T_{LM}^{(n)\dagger}(\alpha)$  are normalized  $\langle 0 | T_{L'M'}^{(n)}(\alpha') T_{LM}^{(n)\dagger}(\alpha) | 0 \rangle = \delta_{\alpha\alpha'} \delta_{LL'} \delta_{MM'}$   $n$ -body creation operators coupled to a total angular momentum  $L$  and magnetic projection  $M$ ,  $T_{LM}^{(n)\dagger}(\alpha) =$

$\sum_{12\dots n} C_{12\dots n}^{LM}(\alpha) a_1^\dagger a_2^\dagger \dots a_n^\dagger$ , here 1 is the s.p. index. The traditional SM approach is limited by the Hamiltonian  $H_2 = H^{(1)} + H^{(2)}$  which is a sum of the s.p.  $n = 1$  and a two-body  $n = 2$  terms. In the two-body part the coefficients  $C_{12}^{LM}$  are proportional to the Clebsch-Gordan coefficients and index  $\alpha$  is uniquely identified by the s.p. levels involved. For  $n > 2$  the index  $\alpha$  must include additional information about the coupling scheme, the choice of which in general is not unique. In numerical work it is convenient to define coefficients  $C_{12\dots n}^{LM}(\alpha)$  and the normalized  $n$ -body operators  $T_{LM}^{(n)}(\alpha)$  using a set of orthogonal eigenstates  $|LM\alpha\rangle = T_{LM}^{(n)\dagger}(\alpha)|0\rangle$  of some  $n$ -particle system, see also [7].

Here we study a single- $j$   $0f_{7/2}$  shell, for past works in this mass region see Refs. [8, 9, 10, 11]. The best experimentally explored systems are  $N = 28$  isotones starting from  $^{48}\text{Ca}$  considered as a core with protons filling the  $0f_{7/2}$  shell and the  $Z=20$   $^{40-48}\text{Ca}$  isotopes with valence neutrons. The experimentally known states identified with the  $f_{7/2}$  valence space are listed in Tab. I.

The three-body interactions influence nuclear masses and result in important monopole terms [4]. The violation of particle-hole symmetry is related to this. Within the traditional SM in a single- $j$  this symmetry makes spectra of  $N$  and  $\tilde{N} = \Omega - N$  particle systems identical apart from a constant shift in energy. Indeed, the particle-hole conjugation  $\mathcal{C}$  defined with  $\tilde{a}_{jm}^\dagger \equiv \mathcal{C} a_{jm}^\dagger \mathcal{C}^{-1} = (-1)^{j-m} a_{j-m}$  transforms an arbitrary  $n$ -body interaction into itself plus some Hamiltonian of a lower interaction-rank  $H'_{n-1}$ , as follows  $\tilde{H}^{(n)} = (-1)^n H^{(n)} + H'_{n-1}$ . The  $n = 1$  case is equivalent to the particle number  $\tilde{N} = -N + \Omega$ . For the  $n = 2$  we obtain a monopole shift

$$\tilde{H}^{(2)} = H^{(2)} + (\Omega - 2N)M, \quad M = \frac{1}{\Omega} \sum (2L+1) V_L^{(2)}. \quad (2)$$

Any  $H^{(1)}$  is proportional to  $N$  and thus is a constant of motion, which explains the particle-hole symmetry for the two-body Hamiltonian. The  $n \geq 3$  interactions violate this symmetry leading to different excitation spectra of  $N$  and  $\tilde{N} = \Omega - N$  particle systems. The deviations from exact particle-hole symmetry are seen in the experimental data, Tab. I. The excitation energies of  $\nu = 2$

		$Z = 28$			$N = 20$		
spin	$\nu$	name	Binding	$3Bf_{7/2}$	name	Binding	$3Bf_{7/2}$
0	0	<sup>48</sup> Ca	0	0	<sup>40</sup> Ca	0	0
7/2	1	<sup>49</sup> Sc	9.626	9.753	<sup>41</sup> Ca	8.360	8.4870
0	0	<sup>50</sup> Ti	21.787	21.713	<sup>42</sup> Ca	19.843	19.837
2	2	1.554	20.233	20.168	1.525	18.319	18.314
4	2	2.675	19.112	19.158	2.752	17.091	17.172
6	2	3.199	18.588	18.657	3.189	16.654	16.647
7/2	1	<sup>51</sup> V	29.851	29.954	<sup>43</sup> Ca	27.776	27.908
5/2	3	0.320	29.531	29.590	.373	27.404	27.630
3/2	3	0.929	28.922	28.992	.593	27.183	27.349
11/2	3	1.609	28.241	28.165	1.678	26.099	26.128
9/2	3	1.813	28.037	28.034	2.094	25.682	25.747
15/2	3	2.700	27.151	27.106	2.754	25.022	24.862
0	0	<sup>52</sup> Cr	40.355	40.292	<sup>44</sup> Ca	38.908	38.736
2	2*	1.434	38.921	38.813	1.157	37.751	37.509
4	4*	2.370	37.986	38.002	2.283	36.625	36.570
4	2*	2.768	37.587	37.643	3.044	35.864	36.009
2	4*	2.965	37.390	37.183	2.657	36.252	35.741
6	2	3.114	37.241	37.353	3.285	35.623	35.606
5	4	3.616	36.739	36.789	-	-	35.180
8	4	4.750	35.605	35.445	(5.088)	(33.821)	33.520
7/2	1	<sup>53</sup> Mn	46.915	47.009	<sup>45</sup> Ca	46.323	46.406
5/2	3	0.378	46.537	46.560	.174	46.149	46.280
3/2	3	1.290	45.625	45.695	1.435	44.888	44.991
11/2	3	1.441	45.474	45.454	1.554	44.769	44.763
9/2	3	1.620	45.295	45.309	-	-	44.933
15/2	3	2.693	44.222	44.175	(2.878)	(43.445)	43.214
0	0	<sup>54</sup> Fe	55.769	55.712	<sup>46</sup> Ca	56.717	56.728,
2	2	1.408	54.360	54.286	1.346	55.371	55.501
4	2	2.538	53.230	53.307	2.575	54.142	54.332
6	2	2.949	52.819	52.890	2.974	53.743	53.659
7/2	2	<sup>55</sup> Co	60.833	60.893	<sup>47</sup> Ca	63.993	64.014
0	0	<sup>56</sup> Ni	67.998	67.950	<sup>48</sup> Ca	73.938	73.846

Table I: States in  $f_{7/2}$  valence space with spin and seniority listed in the first and second columns. The \* denotes seniority mixed states in  $3Bf_{7/2}$ . Following are columns with data for  $N = 28$  isotones and  $Z = 20$  isotopes. Three columns for each type of valence particles list name and excitation energy, experimental binding energy, and energy from the three-body SM calculation discussed in the text. All data is in MeV.

states in  $N = 2$  system are systematically higher than those in the 6-particle case pointing on a reduced ground state binding.

The  $j = 7/2$  is the largest single- $j$  shell for which the number of unpaired nucleons  $\nu$ , the seniority, is an integral of motion for any one- and two-body interaction [10, 12]. It is established experimentally that seniorities are mixed [13, 14]. Configurations beyond the single-

$j$  shell [15, 16] have been suggested to explain the effects, however the possible presence of the three-body force must be addressed. In a single- $j$  the pair operators  $T_{00}^{(2)}$ ,  $T_{00}^{(2)\dagger}$  and the particle number  $N$  form an  $SU(2)$  rotational quasispin group. The quantum numbers  $\nu$  and  $N$  are associated with this group. The invariance under quasispin rotations relates states of the same  $\nu$  but different particle number  $N$ . For example excitation energies of  $\nu = 2$  states are identical in all even-particle systems. In analogy to usual rotations quasispin applies to operators and selection rules. The s.p. operators associated with the particle transfer permit seniority change  $\Delta\nu = 1$ . The reactions  $^{51}\text{V}(^3\text{He}, d)^{52}\text{Cr}$  and  $^{43}\text{Ca}(d,p)^{44}\text{Ca}$  show seniority mixing as  $\nu = 4$  final states are populated [14, 15]. The one-body multipole operators are quasispin scalars for odd angular momentum, and quasispin vectors for even. Thus, the  $M1$  electromagnetic transitions do not change quasispin. In the mid-shell the quasi-vector  $E2$  transitions between states of the same seniority are forbidden. The seniority mixing between  $\nu = 2$  and  $\nu = 4$  pairs of  $2^+$  and  $4^+$  states is expected in the mid-shell nuclei  $^{52}\text{Cr}$  and  $^{44}\text{Ca}$ . Seniority can be used to classify the many-body operators  $T_{LM}^{(n)}$  and interaction parameters. The three-body interactions mix seniorities with the exception of interaction between  $\nu = 1$  nucleon triplets given by the strength  $V_{7/2}^{(3)}$ .

To determine the interaction parameters of  $H_3$  we conduct a full least-square fit to data points in Tab. I. This empirical method which dates back to Refs. [10, 17] is a part of the most successful SM techniques today [18]. Our procedure is similar to a two-body fit in sec. 3.2 of Ref. [19] but here the fit is nonlinear and requires iterations due to seniority mixing. In Tab. II the resulting parameters are listed for the proton  $N = 28$  system and neutron  $Z = 20$  system. The two columns in each case correspond to fits without ( $2Bf_{7/2}$  left) and with ( $3Bf_{7/2}$  right) the three-body forces. The root-mean-square deviation (RMS) is given for each fit. The confidence limits can be inferred from variances for each fit parameter given in brackets.

The lowering of the RMS deviation is the first evidence in support of the three-body forces, for  $Z = 28$  isotones it drops from 120keV to about 80keV. All three-body parameters appear to be equally important, excluding any one of them rises RMS by about 10%. In contrast, inclusion of four-body monopole force based on  $\nu = 0$   $L = 0$  operator led to no improvement. The fit parameters remain stable within quoted error-bars if some questionable data-points are removed. The energies resulting from the three-body fit are listed in Tab. (I). Based on the RMS this description of data is better than what can be achieved with two-body shell models in the expanded model space [20].

The proton and neutron effective Hamiltonians are different, Tab. II. The s.p. energies reflect different mean fields and the two-body parameters especially for higher  $L$  highlight the contribution from the long range

	N=28		Z=20	
	2B $f_{7/2}$	3B $f_{7/2}$	2B $f_{7/2}$	3B $f_{7/2}$
$\epsilon$	-9827(16)	-9753(30)	-8542(35)	-8486.98(72)
$V_0^{(2)}$	-2033(60)	-2207(97)	-2727(122)	-2863(229)
$V_2^{(2)}$	-587(39)	-661(72)	-1347(87)	-1340(176)
$V_4^{(2)}$	443(25)	348(50)	-164(49)	-198(130)
$V_6^{(2)}$	887(20)	849(38)	411(43)	327(98)
$V_{7/2}^{(3)}$		55(28)		53(70)
$V_{5/2}^{(3)}$		-18(70)		2(185)
$V_{3/2}^{(3)}$		-128(88)		-559(273)
$V_{11/2}^{(3)}$		102(43)		51(130)
$V_{9/2}^{(3)}$		122(41)		272(98)
$V_{15/2}^{(3)}$		-53(29)		-24(73)
RMS	120	80	220	170

Table II: Interaction parameters of 2B $f_{7/2}$  and 3B $f_{7/2}$  SM Hamiltonians determined with the least-square fit are given in keV.

Coulomb force. However, within the error-bars the three-body part of the Hamiltonians appears to be the same which relates these terms to isospin invariant strong-force.

A skeptic may question some experimental states included in the fit, thus we conduct a minimal fit considering binding energies of ground states only, similar to the Ref. [10]. We include a seniority conserving part given by  $V_{7/2}^{(3)}$  with  $\nu = 1$  triplet operator  $T_{jm}^{(3)} \sim a_{jm}^\dagger T_{00}^{(2)}$ . This interaction is the main three-body contribution to binding and is equivalent to a density dependent pairing force [21]. In a single- $j$  model it can be treated exactly with a renormalized particle number dependent pairing strength  $V_0^{(2)'} = V_0^{(2)} + \Omega \frac{N-2}{\Omega-2} V_j^{(3)}$ . From relations in Ref. [10, 11] the ground state energies with  $\nu = 0$  or 1 are

$$E = \epsilon N + \frac{N-\nu}{\Omega-2} \left( (\Omega - N - \nu) \frac{V_0^{(2)'}}{2} + (N - 2 + \nu) M' \right), \quad (3)$$

where prime indicates the use of  $N$ -dependent pairing strength. With a linear least-square fit and Eq. (3) we determine s.p. energy  $\epsilon$  pairing  $V_0^{(2)}$ , monopole  $M$ , and 3-body interaction  $V_{7/2}^{(3)}$  (3) using 8 binding energies. The results, shown in Tab III, are consistent with the full fit in Tab. II, the repulsive nature of the monopole  $V_{7/2}^{(3)}$  is in agreement with other works [22].

Next we concentrate on the  $^{52}\text{Cr}$ , Fig.1. In addition to 2B $f_{7/2}$  and 3B $f_{7/2}$  interactions from Tab. II we perform a large scale SM calculation 2B $f_{7/2}p$  (includes  $p_{1/2}$  and  $p_{3/2}$ ) and 2B $fp$  (entire  $fp$ -shell, truncated to  $10^7$  projected m-scheme states) using FPBP two-body SM Hamiltonian [23]. The 2B $f_{7/2}p$  model and its results are very close to more restricted SM calculations in Ref. [20].

	N = 28		Z = 20	
$\epsilon$	-9703(40)	-9692(40)	-8423(51)	-8403(55)
$V_0^{(2)}$	-2354(80)	-2409(110)	-3006(120)	-3105(156)
$M$	1196(40)	1166(50)	-823(55)	-876(76)
$V_{7/2}^{(3)}$	-	18(20)	-	31(31)
RMS	50	46	73	65

Table III: Interaction parameters for the minimal  $f_{7/2}$  SM determined with the linear least-squared fit of 8 binding energies. In brackets the variances for each parameter are shown. The two columns for isotopes and isotones are fits without and with the three-body term.

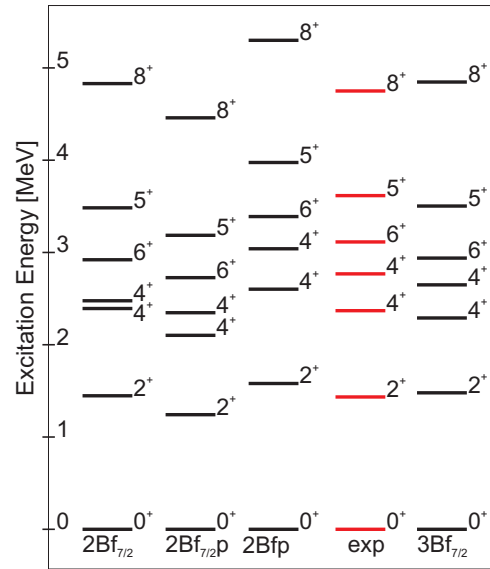


Figure 1: Spectrum of  $^{52}\text{Cr}$ .

The seniority mixing between neighboring  $4_1^+$  and  $4_2^+$  states leads to level repulsion, the observed energy difference of 400 keV is not reproduced by the 2B $f_{7/2}$  (84 keV). The discrepancy remains in the extended two-body models 2B $f_{7/2}p$  and [20] (200 keV). The full 2B $fp$  replicates the splitting at the expense of excessive intruder admixtures which distort the spectrum. The 3B $f_{7/2}$  is best in reproducing the spectrum Fig. 1. The 3B $f_{7/2}$  model predicts seniority mixing, the  $\nu(4_1^+) = 2.82$  and  $\nu(4_2^+) = 2.71$  are inferred from the expectation value of the pair operator  $\langle T_{00}^{(2)\dagger} T_{00}^{(2)} \rangle = (N - \nu)(2j + 3 - N - \nu)/(4j + 2)$ . The  $2_1^+$ , however is relatively pure with  $\nu(2_1^+) = 2.006$ .

Seniority mixing violates quasispin selection rules [9, 13, 14, 24, 25]. The two-body models beyond single- $j$   $f_{7/2}$  break the quasispin symmetry [8, 9, 15, 16, 20], but often fail to exhibit realistic features. To explain electromagnetic transitions large variations of effective charges are needed [26]. The particle transfer spectroscopic factors show excessive amount of components outside the  $f_{7/2}$  valence space [13]. In Tab. IV  $B(E2)$  transitions rates from three models are compared to experiment.

	2B $f_{7/2}$	2B $f_{7/2}p$	2B $fp$	3B $f_{7/2}$	Experiment
$2_1 \rightarrow 0_1^{(*)}$	118.0	118.0	118	117.5	118±35
$4_1 \rightarrow 2_1$	130.4	122.5	105.8	73.2	83±15 <sup>(1,2)</sup>
$4_2 \rightarrow 2_1$	0	3.3	15.1	56.8	69±18
$4_2 \rightarrow 4_1$	125.2	59.3	2.6	0.5	
$2_2 \rightarrow 0_1$	0	0.003	0.9	0.5	0.06±0.05
$2_2 \rightarrow 2_1$	119.2	102.2	101.9	117.1	150±35
$2_2 \rightarrow 4_1$	0	10.8	34.4	19.9	
$2_2 \rightarrow 4_2$	57.8	7.2	5.2	38.7	
$6_1 \rightarrow 4_1$	108.9	86.2	56.3	57.8	59±20 <sup>(1)</sup>
$6_1 \rightarrow 4_2$	0	9.3	27.6	51.1	30±10 <sup>(1)</sup>

Table IV: B(E2) transition summary on  $^{52}\text{Cr}$  expressed in units  $e^2 fm^4$ . The data is taken from [27]. (\*)In 2B  $f_{7/2}p$  and 2B $fp$  models we use 0.5(neutron) and 1.5(proton) effective charges, the overall radial scaling is fixed by B(E2,  $2_1 \rightarrow 0_1$ ). <sup>(1)</sup>The life-time error-bars were used. <sup>(2)</sup>There are conflicting results on life-time we use DSAM (HI,  $xn\gamma$ ) data from Ref. [27], which is consistent with [26].

	2B $f_{7/2}$	2B $f_{7/2}p$	2B $fp$	3B $f_{7/2}$	Exp
$0_1^+$	4.00	3.73	3.40	4.00	4.00
$2_1^+$	1.33	1.14	0.94	1.33	1.08
$4_1^+$	0.00	0.13	0.34	0.63	0.51
$4_2^+$	1.33	1.11	0.70	0.71	0.81
$6_1^+$	1.33	1.28	1.28	1.33	1.31

Table V: Proton removal spectroscopic factors. The experimental data is taken from  $^{51}\text{V}(^3\text{He,d})^{52}\text{Cr}$  reaction [13]. Within error-bars of about 0.1 this data is consistent with other results [27].

The combination of nuclear radial overlap and effective charge is normalized using observed  $E2$  rate for transition  $2_1 \rightarrow 0_1$  in 2B $f_{7/2}$ , 2B $f_{7/2}p$ , and 2B $fp$  models. The parameter for the 3B $f_{7/2}$  model is identical to the one used in 2B $f_{7/2}$ , the insignificant difference in  $2_1 \rightarrow 0_1$  B(E2) between 3B $f_{7/2}$  and 2B $f_{7/2}$  shows a small admixture of  $\nu = 4$  in the  $2_1^+$  state. The  $\nu = 4$  and  $\nu = 2$  mixing in

$4_1^+$  and  $4_2^+$  effects transitions involving these states. For example,  $E2$  transitions  $4_2 \rightarrow 2_1$  and  $6_1 \rightarrow 4_2$  are no longer forbidden. The extended 2B modes improve the picture but not to the quality of the 3B $f_{7/2}$  model.

In Tab. V proton removal spectroscopic factors are compared between theoretical models and experiment  $^{51}\text{V}(^3\text{He,d})^{52}\text{Cr}$  [13]. The 3B $f_{7/2}$  model is again superior in its description of observation especially for the  $4_1^+$  and  $4_2^+$  states. It was pointed in Ref. [13] that spectroscopic factors for  $4^+$  probe the  $\nu = 2$  component, and thus their sum within  $f_{7/2}$  valence space is 4/3, this result is consistent with observation [13] but does support the expanded valence space where spectroscopic factors are naturally reduced.

To conclude, the study of nuclei in  $0f_{7/2}$  shell shows evidence for three-body forces. We extend the traditional shell model approach by including three-body forces into consideration, we find that a successful set of interaction parameters can be determined with an empirical fitting procedure. With a few new parameters a sizable improvement in description of experimental data is obtained. The apparent hierarchy of contributions from one-body mean-field, to two-body, to three-body and beyond is significant; it assures the possibility of high precision configuration-interaction methods in restricted space and supports ideas about renormalization of interactions. The three-body forces observed in this study appear to be isospin invariant. The new Hamiltonian with three-body force, while remaining simple, is superior in its description of spectra, electromagnetic transition rates, and spectroscopic factors compared to the advanced two-body shell model calculations conducted in this work and elsewhere [20]. The work in this direction is to be continued, it is important to conduct similar investigations for other mass regions and model spaces, on the other side renormalization techniques that would link fundamental and phenomenological forces [5] have to be searched for.

The author is thankful to N. Auerbach and V. Zelevinsky for enlightening discussions. Support from the U. S. Department of Energy, grant DE-FG02-92ER40750 is acknowledged.

- 
- [1] S. C. Pieper, V. R. Pandharipande, R. B. Wiringa, and J. Carlson, Phys. Rev. C **64**, 014001 (2001).  
[2] A. van Hees, J. Booten, and P. Glaudemans, Phys.Rev.Lett. **62**, 2245 (1989).  
[3] A. van Hees, J. Booten, and P. Glaudemans, Nucl. Phys. A, **507**, 55 (1990).  
[4] A. P. Zuker, Phys.Rev.Lett. **90**, 042502 (2003).  
[5] A. Schwenk and J. D. Holt (2008), arXiv:0802.3741.  
[6] B. Barrett, D. Dean, M. Hjorth-Jensen, and J. Vary, J. Phys. G **31** (2005).  
[7] A. Volya, Phys. Rev. Lett. **100**, 162501 (2008).  
[8] J. N. Ginocchio and J. B. French, Phys. Lett. **7**, 137 (1963).  
[9] J. D. McCullen, B. F. Bayman, and L. Zamick, Phys.Rev. **134**, B515 (1964).  
[10] I. Talmi, Phys.Rev. **107**, 326 (1957).  
[11] A. Volya, Phys. Rev. C **65**, 044311 (2002).  
[12] C. Schwartz and A. deShalit, Phys.Rev. **94**, 1257 (1954).  
[13] D. D. Armstrong and A. G. Blair, Phys.Rev. **140**, B1226 (1965).  
[14] J. H. Bjerregaard and O. Hansen, Phys.Rev. **155**, 1229 (1967).  
[15] N. Auerbach, Phys. Lett. B, **24**, 260 (1967).  
[16] T. Engeland and E. Osnes, Phys. Lett. **20**, 424 (1966).  
[17] R. F. Bacher and S. Goudsmit, Phys.Rev. **46**, 948 (1934).  
[18] B. A. Brown and W. A. Richter, Phys. Rev. C **74**, 034315

- (2006).
- [19] R. D. Lawson, *Theory of the nuclear shell model* (Clarendon Press, 1980).
- [20] K. Lips and M. T. McEllistrem, *Phys.Rev.C* **1**, 1009 (1970).
- [21] V. Zelevinsky, T. Sumaryada, and A. Volya (2006), <http://meeting.aps.org/link/BAPS.2006.APR.C8.4>.
- [22] S. A. Coon, M. T. Pena, and D. O. Riska, *Phys.Rev.C* **52**, 2925 (1995).
- [23] B. A. Brown, *Progress in Particle and Nuclear Physics* **47**, 517 (2001).
- [24] C. F. Monahan, et.al., *Nucl. Phys. A*, **120**, 460 (1968).
- [25] F. Pellegrini, I. Filosofo, M. I. E. Zaiki, and I. Gabrielli, *Phys.Rev.C* **8**, 1547 (1973).
- [26] B. A. Brown, D. B. Fossan, J. M. McDonald, and K. A. Snover, *Phys.Rev.C* **9**, 1033 (1974).
- [27] J. Huo, S. Huo, and C. Ma, *Nuclear Data Sheets*, **108**, 773 (2007).